Annals of Botany **130**: 671–685, 2022
https://doi.org/10.1093/aob/mcac117, available online at www.academic.oup.com/aob

ANNALS OF BOTANY
Founded 1887

Phylotranscriptomics reveal the spatio-temporal distribution and morphological evolution of *Macrozamia*, an Australian endemic genus of Cycadales

Sadaf Habib[1,2], Yiqing Gong[1], Shanshan Dong[1], Anders Lindstrom[3], Dennis William Stevenson[4], Yang Liu[1,], Hong Wu[2,] and Shouzhou Zhang[1,*]

[1]Key Laboratory of Southern Subtropical Plant Diversity, Fairy Lake Botanical Garden, Shenzhen & Chinese Academy of Sciences, Shenzhen, 518004, China, [2]College of Life Sciences, South China Agricultural University, Guangzhou, 510642, China, [3]Global Biodiversity Conservancy 144/124 Moo 3, Soi Bua Thong, Bangsalae, Sattahip, Chonburi 20250, Thailand, and [4]New York Botanical Garden, Bronx, NY 10458, USA
** For correspondence. E-mail shouzhouz@szbg.ac.cn*

Received: 12 May 2022 Returned for revision: 4 September 2022 Editorial decision: 8 September 2022 Accepted: 14 September 2022
Electronically published: 16 September 2022

• **Background and Aims** Cycads are regarded as an ancient lineage of living seed plants, and hold important clues to understand the early evolutionary trends of seed plants. The molecular phylogeny and spatio-temporal diversification of one of the species-rich genera of cycads, *Macrozamia*, have not been well reconstructed.
• **Methods** We analysed a transcriptome dataset of 4740 single-copy nuclear genes (SCGs) of 39 *Macrozamia* species and two outgroup taxa. Based on concatenated (maximum parsimony, maximum likelihood) and multispecies coalescent analyses, we first establish a well-resolved phylogenetic tree of *Macrozamia*. To identify cyto-nuclear incongruence, the plastid protein coding genes (PCGs) from transcriptome data are extracted using the software HybPiper. Furthermore, we explore the biogeographical history of the genus and shed light on the pattern of floristic exchange between three distinct areas of Australia. Six key diagnostic characters are traced on the phylogenetic framework using two comparative methods, and infra-generic classification is investigated.
• **Key Results** The tree topologies of concatenated and multi-species coalescent analyses of SCGs are mostly congruent with a few conflicting nodes, while those from plastid PCGs show poorly supported relationships. The genus contains three major clades that correspond to their distinct distributional areas in Australia. The crown group of *Macrozamia* is estimated to around 11.80 Ma, with a major expansion in the last 5–6 Myr. Six morphological characters show homoplasy, and the traditional phenetic sectional division of the genus is inconsistent with this current phylogeny.
• **Conclusions** This first detailed phylogenetic investigation of *Macrozamia* demonstrates promising prospects of SCGs in resolving phylogenetic relationships within cycads. Our study suggests that *Macrozamia*, once widely distributed in Australia, underwent major extinctions because of fluctuating climatic conditions such as cooling and mesic biome disappearance in the past. The current close placement of morphologically distinct species in the phylogenetic tree may be related to neotenic events that occurred in the genus.

Key words: Cycadales, *Macrozamia*, biogeography, phylotranscriptomics, character evolution, gymnosperms.

INTRODUCTION

Cycads, with ten extant genera, are regarded as one of the first branching lineages of seed plants (Brenner *et al.*, 2003*a*). They have a long evolutionary history holding important clues to understand early evolutionary trends of seed plants such as the origin and evolution of cones, seeds and plant vegetative structures (Brenner *et al.*, 2003*a*, b; Salas-Leiva *et al.*, 2013; Zumajo-Cardona *et al.*, 2021*a*, b). Thus, it is important to understand the evolutionary trends and phylogenetic relationships among taxa, and contribute towards their conservation. Unfortunately, nearly 63 % of extant cycads worldwide are threatened by extinction due to habitat destruction and degradation, and are included in the International Union for Conservation of Nature (IUCN) Red List of Threatened Plants (IUCN, 2022). Phylogenetic relationships within cycads have been highlighted previously for several genera (Caputo *et al.*, 2004; Treutlein *et al.*, 2005; De Castro *et al.*, 2006; González *et al.*, 2008; Xiao *et al.*, 2010; Moynihan *et al.*, 2012; Clugston *et al.*, 2016; Gutiérrez-Ortega *et al.*, 2018; J. Liu *et al.*, 2018, 2022; Calonje *et al.*, 2019; Medina-Villarreal *et al.*, 2019; Mankga *et al.*, 2020). However, the phylogenetic relationships within one of the most species-rich genera of cycads, *Macrozamia*, have not been well studied. There are 41 species of *Macrozamia* endemic to subtropical and warm-temperate areas of Australia, and which are usually found on arid soils in sclerophyll communities (Hill and Osborne, 2001; Osborne *et al.*, 2012).

Molecular phylogenetic relationships within *Macrozamia* are unresolved as no extensive studies have focused on this genus. Sangin *et al.* (2008) studied the phylogenetic relationships within Zamiaceae based on a chloroplast DNA (cpDNA) (non-coding *trnS-trnG*) region. Their study included only 11 species of *Macrozamia*, but did not obtain any well-supported

phylogenetic relationships within the genus. Ingham *et al.* (2013) sequenced two chloroplast intergenic regions (*atpH-atpI* and *trnL-trnF*) for all the described species of *Macrozamia* and focused on the biogeographical distribution of species among distinct areas based on their haplotype network.

Macrozamia is restricted primarily to eastern Australia with only three species reported from south-western Australia and one species recognized from central Australia (Ingham *et al.*, 2013). Using the extrapolation of the crown group age from Crisp and Cook (2011), Ingham *et al.* (2013) concluded that the diversification of *Macrozamia* species from eastern to western Australia occurred about 6 Ma. Moreover, the only species of *Macrozamia* in central Australia (*Macrozamia macdonnellii*) was isolated from species in eastern Australia by an event occurring in the Pleistocene (Ingham *et al.*, 2013). However, because of the low level of cpDNA divergence between species, investigations based on reliable phylogenetic reconstructions with an extensive dataset and significant informative characters are required to explore the diversification pattern of species within the genus. Therefore, a detailed exploration of the molecular phylogeny and investigation of spatio-temporal diversification of the genus *Macrozamia* is required.

The spatio-temporal dynamics of the genus is of particular importance for pollination biology as *Macrozamia* species have an obligate pollination mutualism with their obligate thrips pollinators in the genus *Cycadothrips* (Thysanoptera, family Aeolothripidae), weevils within the genus *Tranes* (Coleoptera, family Curculionidae) or the genus *Paracucujus* (Coleoptera, family Boganiidae). Additionally, a few species are pollinated by both *Cycadothrips* and *Tranes* (Jones *et al.*, 2001; Mound and Terry, 2001; Terry *et al.*, 2007, 2014; Cai *et al.*, 2018). Mapping of functional traits responsible for such mutualism onto comprehensive phylogenies of these tightly associated mutualistic organisms would allow further inference into the processes responsible for their co-diversification. The spatio-temporal diversification pattern of the genus *Macrozamia* revealed in the present study we hope will lay the foundation for extensive studies, for example those regarding obligate pollination mutualism among these mutualistic organisms (Brookes *et al.*, 2015).

Based on leaf morphology, Hill (1998) divided the then recognized 38 species into two sections: *M.* sect. *Macrozamia* and *M.* sect. *Parazamia*. *Macrozamia* sect. *Macrozamia* (15 species) is characterized by large plants with 12–150 leaves in the crown; pinnae thin, veins visible on leaves, sometimes raised on the lower surface when dry; mucilage canals present in pinnae; and lower pinnae reduced to spines. In contrast, *M.* sect. *Parazamia* (23 species) comprises small plants with 1–15 leaves in the crown; thick and prominent veins on the lower surface, especially when dry; mucilage canals absent in pinnae; and lower pinnae not reduced to spines. Furthermore, closely related species were also assigned as species complexes within each section of *Macrozamia*, based on their morphology and adjacent geological proximity (Jones and Forster, 1994; Hill and Osborne, 2001; Jones *et al.*, 2001; Forster, 2004). Morphological features of *Macrozamia* are presented in Fig. 1. Isozyme investigations indicated low to high genetic diversity among the species within these complexes (Sharma *et al.*, 1998,

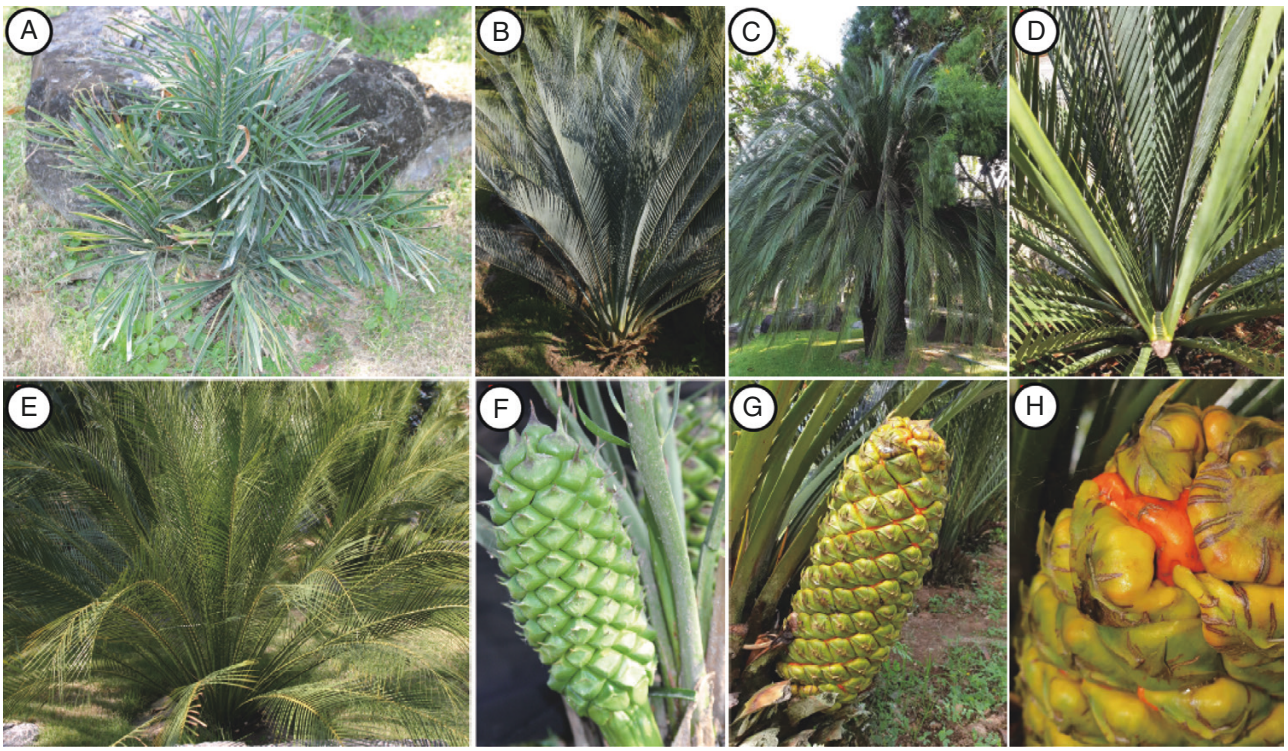

FIG. 1. Morphological diversity of *Macrozamia.* (A) Subterranean plant of *M. lomandroides* with fewer leaves in a crown; (B) small arborescent stem of *M. macdonnellii* with several blue-green leaves arranged in a crown; (C) arborescent stem of *M. moorei*; (D) keeled leaves of *M. macdonnellii*; (E) flat leaves of *M. johnsonii*; (F) male cone of *M. crassifolia*; (G, H) female cone of *M. miquelii* with orange-red seed. Photographs by A. Lindstrom.

1999*a*, b, 2004). The sectional classification and phylogenetic placement of *Macrozamia* species required detailed investigation based on a reliable phylogenetic framework using new molecular data combined with existing data and approaches (Daly *et al.*, 2001).

Phylogenetic analyses based on transcriptome sequences have proved to be efficient and cost-effective (Leebens-Mack *et al.*, 2019; Stull *et al.*, 2021). Recent studies have demonstrated the utility of transcriptome data for resolving the relationships among several seed plant groups (J. Wen *et al.*, 2013, 2020; Yang *et al.*, 2014; Dorsey *et al.*, 2018). Furthermore, transcriptome data have also been extensively used for exploring character evolution, possible hybridization events and biogeographical history (Ali *et al.*, 2020; C. Zhang *et al.*, 2021; Y. Y. Liu *et al.*, 2022). Given the potential significance of transcriptome-based phylogenomics, the present study uses this approach to resolve the deep relationships within the genus *Macrozamia*. The spatial and temporal diversification of the genus is then analysed based on our well-resolved phylogenetic framework and reliable fossil evidence. Finally, evolution of key morphological characters is traced to test the section-based classification and species complexes of *Macrozamia* within the phylogenetic framework.

MATERIALS AND METHODS

Sampling, sequencing and transcriptome data retrieval

Forty-one raw sequences were obtained from our research project on the *Cycas* genome, investigated with whole genome of *Cycas panzhihuaensis*, complemented by the transcriptomes of 339 cycad species (Y. Liu *et al.*, 2022). Our in-group sampling consists of 39 *Macrozamia* and two outgroup representative taxa from the sister genera *Lepidozamia* and *Encephalartos*. Among these 41 accessions, 40 were newly sampled in Y. Liu *et al.*, (2022), and one species (*M. macdonnellii*) was newly added in this study. These species were collected from the Nong Nooch Tropical Botanical Garden, Pattaya, Thailand (NNTBG). The voucher specimens were deposited at Bangkok Herbarium (BK), Thailand, and Natural History Museum (W), Austria (Table 1).

The raw sequencing reads were trimmed and filtered for adaptors, low quality and duplicate reads, using Trimmomatic (https://github.com/timflutre/trimmomatic). The cleaned transcriptome reads were *de novo* assembled using the Trinity pipeline (Grabherr *et al.*, 2011). From the assembled transcriptomes, the longest transcripts were selected and annotated with TransDecoder (https://github.com/TransDecoder). Annotated transcripts were then subjected to orthology detection using OrthoFinder (Emms and Kelly, 2019). The software KinFin (Laetsch and Blaxter, 2017) was used to select the mostly single copy genes (SCGs) for phylogenetic reconstruction with default settings. SCGs present in more than 70 % of the taxa were selected for subsequent phylogenomic analyses. The dataset of each gene was filtered to keep only SCGs and aligned using a local version of the program TranslatorX (Abascal *et al.*, 2010). Briefly, the nucleotide sequences were first translated into an amino acid sequence using the standard genetic code, and then an amino acid alignment was created by using MAFFT (Katoh and Standley, 2013). Ambiguous portions in the alignment were trimmed by Gblocks (Talavera and Castresana, 2007) with the least stringent settings. The cleaned amino acid alignment was then used as a guide to generate the alignment for nucleotide sequences for further concatenation- and coalescent-based phylogenetic inferences. Clean RNA-sequencing (RNA-seq) reads of 41 species have been submitted to GenBank under the BioProject ID PRJNA809119.

Phylotranscriptomic analyses

For different SCG datasets, i.e. nucleotide data including all codon positions (nt), nucleotide data from first and second codon position (nt 12) and amino acid alignments (aa), we used both coalescent and supermatrix approaches for analysis. For supermatrix analyses, the final alignments for individual genes were concatenated into combined nucleotide datasets with SeqKit (Shen *et al.*, 2016). The best maximum likelihood (ML) tree for the concatenated nucleotide dataset was constructed using IQ-TREE 2 (Minh *et al.*, 2020), with ultra-fast bootstrap analysis of 1000 replicates. ModelFinder (Kalyaanamoorthy *et al.*, 2017) was used to specify the best-fit nucleotide substitution models, as implemented in IQ-TREE 2. We extracted the variable sites of the complete dataset using a custom perl script (provided on request). The resultant dataset was used for maximum parsimony (MP) analysis, conducted in PAUP 4.0 b10 (Swofford, 2003), with a heuristic search strategy followed by random addition starting trees with options of tree-bisection-reconnection (TBR) branch swapping, and MulTrees selected. Gaps were treated as missing data. Bootstrap values (BS) were obtained from 1000 replicates of heuristic searches as described above (TBR branch swapping, and MulTrees selected), with ten random addition-sequence replicates. (Fig. 2A)

For multi-species coalescent-based analyses, individual gene trees were constructed using IQ-TREE 2, following the same procedure mentioned for the concatenated dataset. These individual unrooted gene trees were then used as input data to estimate species trees using ASTRAL-III (C. Zhang *et al.*, 2018). This program maximizes the number of quartet trees shared between the species tree and the gene trees. The option '-t 8' was used to calculate quartet support (q) for each branch including the main topology and the first and second alternatives. To investigate ambiguously inferred relationships, we used the software SplitsTree5 (Huson, 1998; Huson and Bryant, 2006). The dataset containing variable sites of SCGs for 39 *Macrozamia* species was used as the input data to infer the neighbour-net phylogenetic networks based on uncorrected P distances.

To identify the cyto-nuclear phylogenies of *Macrozamia*, the plastid protein-coding genes (PCGs) were extracted from transcriptome data using HybPiper (Johnson *et al.*, 2016), with the plastid protein coding sequences from available gymnosperms as baits. The resultant datasets were aligned using MAFFT (Katoh and Standley, 2013), and imported into Geneious v.10.0.2 (https://www.geneious.com) for manually checking. Prior to concatenation, genes <200 bp in length and <50 % representative species were removed. An ML tree was constructed for the concatenated plastid dataset in RAxML v.8 (Stamatakis,

TABLE 1. *Information on the 41 transcriptome datasets for 39* Macrozamia*, one* Encephalartos *and one* Lepidozamia *species investigated in this study.*

Taxon name	Voucher accession no.	NCBI accession no.	Clean reads/raw reads (Gb)	Unigene no.	min_len (bp)	avg_len (bp)	max_len (bp)
M. cardiacensis	BK 083982	SRR18094554	4.22/6	29 562	150	1206	17 082
M. communis	BK 083983	SRR18094553	4.06/6	28 802	150	1159.8	13 683
M. conferta	BK 083984	SRR18094542	4.20/6	28 459	150	1225.5	11 808
M. cranei	BK 083985	SRR18094531	4.22/6	31 467	150	1191.6	15 669
M. crassifolia	BK 083986	SRR18094520	4.05/6	31 855	150	1136.4	11 781
M. diplomera	BK 083987	SRR18094518	4.26/6	27 674	150	1258.5	16 476
M. douglasii	BK 083988	SRR18094517	4.21/6	30 210	150	1186.2	17 082
M. dyeri	BK 084010	SRR18094516	3.98/6	28 748	150	1152.3	11 466
M. elegans	BK 083989	SRR18094515	4.16/6	27 965	150	1215.3	12 579
M. fawcettii	W 20120010308	SRR18094514	4.20/6	27 546	150	1218.9	11 778
M. fearnsidei	W 20120010301	SRR18094552	4.01/6	32 459	150	1174.5	12 693
M. flexuosa	BK 083990	SRR18094551	4.00/6	28 644	150	1218	11 532
M. fraseri	BK 084011	SRR18094550	3.86/6	27 559	150	1157.7	11 469
M. glaucophylla	BK 083991	SRR18094549	4.53/6	32 176	150	1168.2	13 683
M. heteromera	BK 083992	SRR18094548	4.00/6	27 756	150	1185.6	11 466
M. humilis	BK 083993	SRR18094547	4.49/6	25 856	150	1263.6	14 265
M. lomandroides	W 20120010108	SRR18094546	4.20/6	28 967	150	1086.9	11 778
M. longispina	W 20120010306	SRR18094545	4.03/6	28 668	150	1187.7	11 778
M. lucida	BK 083994	SRR18094544	4.13/6	30 133	150	1192.5	11 778
M. macdonnellii	BK 083995	SRR18094543	3.92/6	16 446	150	1014	11 376
M. machinii	BK 083996	SRR18094541	4.08/6	31 294	150	1180.8	15 654
M. macleayi	W 20120010297	SRR18094540	4.17/6	31 729	150	1167	15 669
M. miquelii	BK 083997	SRR18094539	4.58/6	24 997	150	1236.6	11 985
M. montana	BK 083998	SRR18094538	4.07/6	27 715	150	1236	17 082
M. moorei	BK 083999	SRR18094537	4.37/6	34 133	150	1164.3	14 640
M. mountperriensis	W 20120010307	SRR18094536	4.11/6	30 529	150	1130.7	11 778
M. parcifolia	W 20120010311	SRR18094535	4.25/6	28 702	150	1207.2	11 778
M. pauli-guilielmi	W 20120010310	SRR18094534	3.85/6	25 950	150	1176.3	11 778
M. platyrhachis	BK 084000	SRR18094533	3.96/6	25 124	150	1225.2	11 466
M. plurinervia	BK 084001	SRR18094532	4.26/6	28 303	150	1178.4	13 749
M. polymorpha	BK 084002	SRR18094530	4.12/6	28 348	150	1210.8	12 567
M. reducta	BK 084003	SRR18094529	4.39/6	23 511	150	1258.5	11 466
M. riedlei	BK 084004	SRR18094528	3.98/6	26 715	150	1243.8	15 555
M. secunda	BK 084005	SRR18094527	3.99/6	28 205	150	1126.8	11 466
M. serpentina	W 20120010312	SRR18094526	4.25/6	27 589	150	1244.7	14 514
M. spiralis	BK 084006	SRR18094525	4.3/6	28 205	150	1197.9	11 976
M. stenomera	BK 084007	SRR18094524	4.6/6	29 550	150	1239.6	13 683
M. viridis	BK 084008	SRR18094523	3.93/6	30 166	150	1183.2	11 778
M. johnsonii	BK 084009	SRR18094522	8.5/12	55 003	255	612.3	13 332
E. longifolius	BK 084012	SRR18094521	8.85/12	70 238	255	591.3	12 198
L. hopei	BK 084013	SRR18094519	4.16/6	80 589	255	558.3	15 537

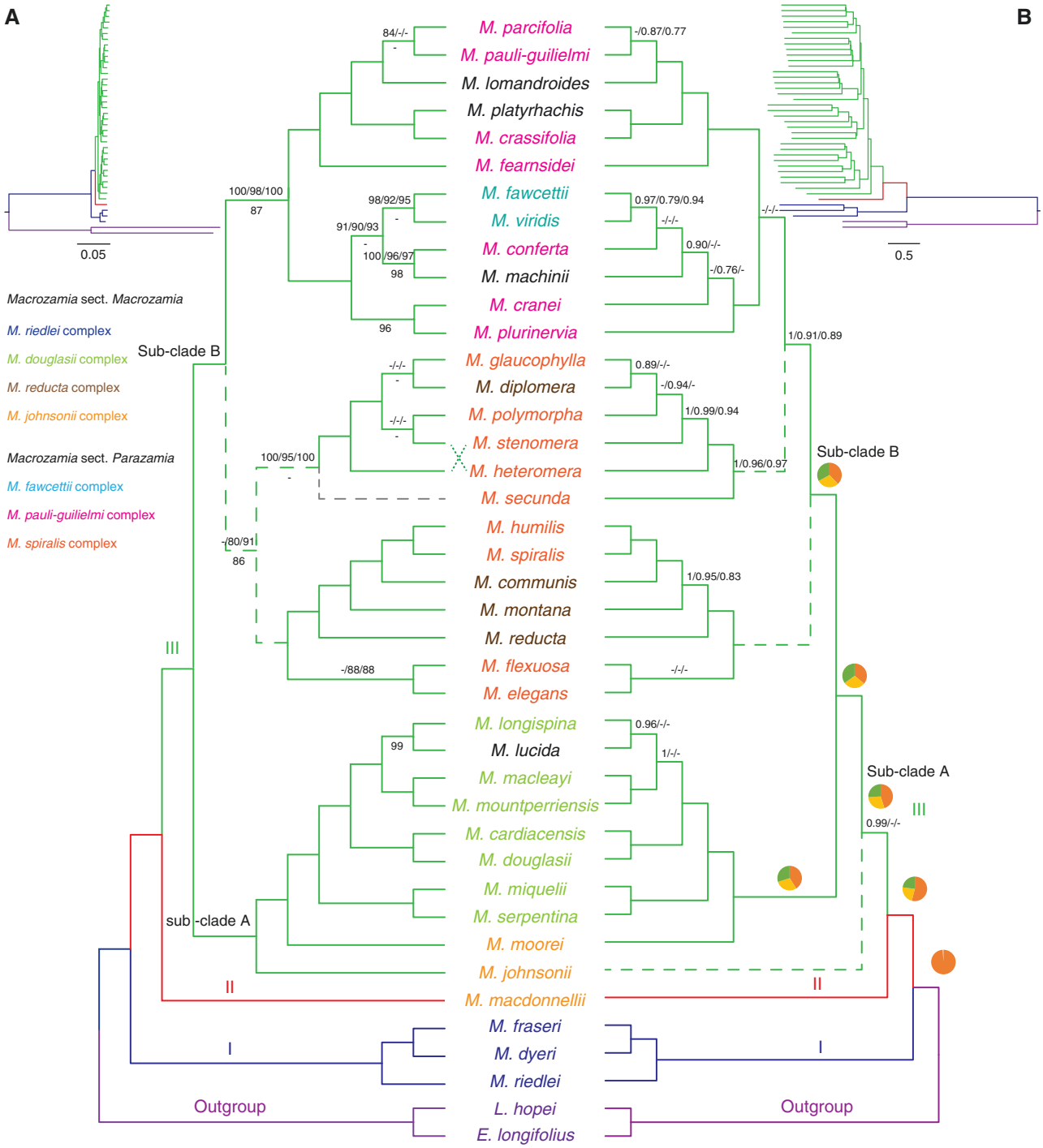

FIG. 2. Phylogenetic tree of the genus *Macrozamia* based on a transcriptome dataset of 4740 single copy nuclear genes (SCGs). (A) ML tree inferred from the concatenated dataset; ML and MP bootstrap (BS) support values are given above (nt/nt12/aa) and below the branches, respectively, if not maximally supported; '–' indicates BS < 75 %. Grey dashed lines indicate incongruence among the ML and MP trees. (B) Species tree generated using ASTRAL-III based on 4740 single copy gene trees. Posterior probability (PP) values are given above branches (nt/nt12/aa), if not maximally supported; '–' indicates PP < 0.75; the pie charts on major clades show respective quartet support for the main topology, and the first and the second alternative topology. Branch colours correspond to three major clades within *Macrozamia*. Taxon colours highlight the position of sections and species complexes within the genus. Coloured dashed lines indicate incongruence among the ML and ASTRAL-III trees.

2014), with the GTR + G substitution model with 100 bootstrap replicates.

Molecular dating and ancestral area reconstruction

Because individual gene trees might show incongruent phylogenetic signal, which affects dating analyses, we carefully checked the individual gene trees and selected 50 genes that produced a congruent tree topology with the species tree for dating analyses. Moreover, these 50 genes have higher species coverage, a threshold of >50 % and sufficient nucleotide divergence. 50-gene ML tree was first constrained to the tree topologies derived from concatenated, multi-species coalescent analyses in RAxML, following the same analytical procedure mentioned for the plastid dataset. The resultant 50-gene trees were used to calculate divergence times using the penalized likelihood method in TreePL (Sanderson, 2002; Smith and O'Meara, 2012). The most recent molecular dating analyses of cycads were performed by Y. Liu *et al.* (2022), based on transcriptome data, using six fossils for the cycad species tree that mainly derived from Condamine *et al.* (2015). Three fossil calibration points used for estimating the age of each tree were as follows: the first calibration point was placed at the stem node of *Lepidozamia* (range: 33.9–265.1 Ma; K. D. Hill, 1998). The second and third points were constrained to the crown age of *Macrozamia* (range: 7.2–11.9 Ma), and root of the Encephalarteae (range: 46.2–69.1 Ma) following Y. Liu *et al.* (2022). The resultant 100 calibrated trees from treePL were used as input for constructing maximum clade credibility (MCC) trees with median ages and 95 % highest posterior density (HPD) intervals on nodes using TreeAnnotator v.2.6.2 (Helfrich *et al.*, 2018). The final results were visualized in FigTree v.1.4.4 (http://tree.bio.ed.ac.uk/software/figtree/). ML estimates of branch-specific substitution rates were calculated with HyPhy v.2.0 (Pond *et al.*, 2005) under the MG94W9 codon model (Muse and Gaut, 1994) and allowing for independent estimation of nonsynoymous (d_N) and synonymous (d_S) substitution values for each branch (the local parameters option) following Richardson *et al.* (2013) and by using the concatenated nucleotide data matrix (excluding outgroups) and the corresponding ML tree inferred from the concatenated nucleotide dataset with IQ-TREE 2 as previously described. The absolute rate of silent substitutions for *Macrozamia* was calculated by dividing the total synonymous substitutions accumulated by the crown age (in billions of years) of the genus.

Distribution data for *Macrozamia* species were compiled based on herbarium records in Australia's Virtual Herbarium (AVH, https://avh.ala.org.au/#tab_simpleSearch), and online Global Biodiversity Information Facility (GBIF, http://www.gbif.org/). We used the R package 'BioGeoBEARS' (Matzke, 2018) to estimate the ancestral range states of the *Macrozamia* species and reconstruct biogeographical histories of the lineages. Areas of endemism were applied to reveal the exchange pattern between four phylogeographical distribution areas of *Macrozamia*, namely A: south-west western Australia, B: central Australia, C: New South Wales (eastern Australia) and D: Queensland (eastern Australia). Eastern, western and central Australia are three well-separated bioregions of Australia. In *Macrozamia*, all but four species are distributed in eastern Australia. While studying the historical biogeography of Australian Rhamnaceae, Ladiges *et al.* (2005) divided eastern Australia into three bioregions (i.e. Queensland, McPherson-Macleay and New South Wales). McPherson-Macleay is the region between Queensland and New South Wales, but the southern boundary of this region is not distinct. Thus, we modified this three bio-region approach into two bio-regions congruent with Queensland and New South Wales states based on the distinct diversification pattern of *Macrozamia* species within these areas and with limited dispersals occurring between them.

Three basic models, i.e. DEC, DIVALIKE and BAYAREALIKE, were tested in BioGeoBEARS, with or without the 'jump dispersal' parameter j, which weights founder-event speciation in the evolutionary estimation. After selecting the optimal model using the Akaike Information Criterion (AIC), the most likely ancestral range reconstructions at each node were extracted and identified for dispersal events on the phylogeny where range expansions or shifts occurred between the ancestor and offspring nodes of a branch.

Character state reconstruction

We traced the evolution of six diagnostic morphological traits of interest reported in previous studies (Hill and Osborne, 2001) over the molecular phylogeny: **1.** Stem: (0) subterranean (1) small arborescent (2) arborescent; **2.** Stomatal distribution: (0) amphistomatic (1) hypostomatic; **3.** Number of leaves in a crown: (0) ≥ 12 (1) < 12; **4.** Pinnacanth formation (basal pinnae reduction to spines): (0) absent (1) present; **5.** Leaf surface: (0) flat (1) keeled; **6.** Seed colour: (0) red (1) orange-red (2) orange. Character states were coded with some modifications that mainly followed K. D. Hill (1998) and Hill and Osborne (2001). For stem arborescence, we described three alternative states (subterranean vs. small arborescent vs. arborescent) instead of two (subterranean vs. arborescent). Species with no trunk, trunk < 0.6 m and trunk > 0.6 m were coded as subterranean, small arborescent and arborescent, respectively. For leaf surface, two alternative states, flat vs. keeled, were used instead of the multiple states, flat vs. slightly keeled vs. moderately keeled vs. strongly keeled, used by K. D. Hill (1998) and Hill and Osborne (2001). This change was done because several species were observed to be polymorphic (e.g. *Macrozamia conferta* and *M. polymorpha*) within the keeled types. The detailed character matrix was completed with data from literature resources (K. D. Hill, 1998; Hill and Osborne, 2001; Jones *et al.*, 2001).

The character states were optimized onto the tree generated from the ML analysis of the concatenated dataset in Mesquite v.3.70 (Maddison and Maddison, 2021) using the ML criterion with Markov k-state one-parameter (Mk1) model (Lewis, 2001), and also in R using the package 'ape' with the function *ace* (Paradis *et al.*, 2004). Prior to ancestral state reconstruction in R, likelihood ratio test (LRT) analysis was performed to test the three different evolutionary models: the ER model (equal rates), the SYM model (symmetrical) and the ARD model (all-rates-different). The best fitting model with the lowest AIC score was selected to infer the ancestral states for each character.

RESULTS

Phylogenetic reconstruction based on transcriptome sequencing

In total, 6–12 Gb of transcriptome data were generated for each of 41 species representing 39 of 41 species of *Macrozamia* (the two missing species are *Macrozamia concinna* and *M. occidua*), and two outgroup species (Table 1). We identified 4740 shared SCGs for the phylogenetic reconstruction of *Macrozamia* with an average alignment length of ~5000 bp and with missing data ranging from 0 % to 31.71 %. The aligned length of the concatenated dataset was 6 018 478 bp with 153 656 (2.50 %) variable sites and 69 020 (1.15 %) parsimony-informative sites. To construct the plastid data matrix, plastid PCGs from all 41 species were extracted from the transcriptome data. After excluding genes <200 bp in length and with <50 % species coverage, the final dataset consisted of 40 plastid PCGs with an aligned length of the concatenated dataset of 33 651 bp and with 2174 (6.4 %) variable sites, 490 (1.45 %) parsimony-informative sites and 31.34 % missing data. Furthermore, we screened out 50 SCGs for a divergence time estimation with higher species coverage with a threshold of >50 % and sufficient nucleotide divergence. The final alignment of these 50 concatenated SCGs was about 52 kb.

The ML tree topologies produced from the concatenated analyses (nt, nt12, aa) were highly concordant (Fig. 2A). MP analysis generated a topology that is similar to the ML tree with no well-supported (>75 % bootstrap support) conflicts detected, except for the position of *Macrozamia secunda* (Fig. 2A). In the multi-species coalescent analyses in ASTRAL-III, no discordance was observed in some of the inferred relationships between analyses of nt, nt12 and aa matrices (Fig. 2B). These relationships revealed that the nt12 and aa topologies were not well supported as compared to the nt tree topologies (Fig. 2B). Furthermore, well-supported conflict among gene histories and the species history was found for some topologies in our phylogenetic reconstructions of SCGs (Fig. 2). the phylogenetic ML tree, based on a concatenated dataset of 40 plastid PCGs, yielded poorly supported topologies (Supplementary Data Fig. S1). Therefore, in the following discussion, we focus on the results from the MP and ML analyses of supermatrix (hereafter MP-con and ML-con) and multi-species coalescent analyses (hereafter MS-col) of SCGs.

Relationships among major lineages of Macrozamia

Based on MP-con, ML-con and MS-col analyses, the genus *Macrozamia* is divided into three well-supported major clades (MP bootstrap = 100 %; ML bootstrap = 100 %; MS posterior probabilities = 1; Fig. 2). Quartet analysis in ASTRAL-III also indicated higher support values for the main topology (q1) as compared to their first and second alternatives (q2 and q3) of all three major clades (Fig. 2B and Supplementary Data Fig. S2). The phylogeny of *Macrozamia* corresponded to its species distribution among the three distinct biogeographical regions of Australia. Three species from western Australia, i.e. *Macrozamia dyeri*, *M. fraseri* and *M. riedlei*, formed a monophyletic group, sister to all remaining taxa of *Macrozamia*, followed by clade II with *M. macdonnellii*, the sole species from central Australia. Clade III is the largest, including 35 species distributed in eastern Australia. Although the phylogenetic relationship among these major clades is consistent and maximally supported, discrepancy occurred within clade III. ML-con approaches revealed that clade III comprised two distinct and highly supported monophyletic groups (BS 100 %) with *Macrozamia johnsonii* included within one of them and with maximum support (BS 100 %). In contrast, based on our MS-col analyses (PP 0.99), *M. johnsonii* is recovered to be the first diverging species within clade III and sister to a monophyletic group of all other remaining taxa. Quartet support analysis in ASTRAL-III indicated considerable gene tree conflict around this branch (q1 = 0.36, q2 = 0.29, q3 = 0.35; Fig. 2B and Supplementary Data Fig. S2). Clade III species were divided into two sub-clades, i.e. sub-clade A (including *M. johnsonii*) and sub-clade B. Based on their morphological affinities, these correspond to *M.* sect. *Macrozamia* and *M.* sect. *Parazamia*, respectively. Phylogenetic relationships within sub-clade A were highly consistent except for the aforementioned conflict concerning *M. johnsonii*. Species of sub-clade B were divided into four well-supported monophyletic groups. The phylogenetic relationships of these groups within sub-clade B are poorly to moderately supported and are inconsistent with our MP-con, ML-con and MS-col analyses (Fig. 2).

Splits graphs retrieved from the concatenated dataset containing variable sites of SCGs revealed a clear clustering of major clades of *Macrozamia* (Supplementary Data Fig. S3). However, significant alternative splits were found, mainly in sub-clade B, which represents an uncertainty in the phylogenetic placement of these taxa. Also, the conflicting position of *M. johnsonii* is evident because this species was placed close to sub-clade A and in between sub-clade A and sub-clade B.

Biogeography and divergence times

Given the considerable gene tree conflict among diverging groups of ML-con and MS-col analyses, we constrained the 50-gene ML tree to the topologies derived from both of these analyses. The resultant trees were then subjected to further diversification analyses, which revealed almost the same findings. The divergence times of *Macrozamia* and its major clades as estimated based on three calibrations are presented in Fig. 3, for topologies derived from ML-con and MS-col analyses. Based on the ML-con time tree, the crown group of *Macrozamia* diversified by 11.77 Ma [95 % highest posterior density (HPD): 11.49–11.9 Ma, node 0] during the late Miocene (Fig. 3A). Clade I began its diversification at around 5.67 Ma (95 % HPD: 4.81–6.60 Ma; node 1) and the divergence between the central (clade II) and the eastern Australia species (clade III) occurred at 8.77 Ma (95 % HPD: 8.24–9.24 Ma; node 2). The crown of clade III was estimated to have diversified 6.85 Ma (95 % HPD: 6.28–7.52 Ma; node 3). The divergence time estimation based on MS-col time showed similar results, except for *M. johnsonii*. The split of *M. johnsonii* from the remaining clade III taxa occurred around 6.46 Ma (95 % HPD: 5.83–7.00 Ma,

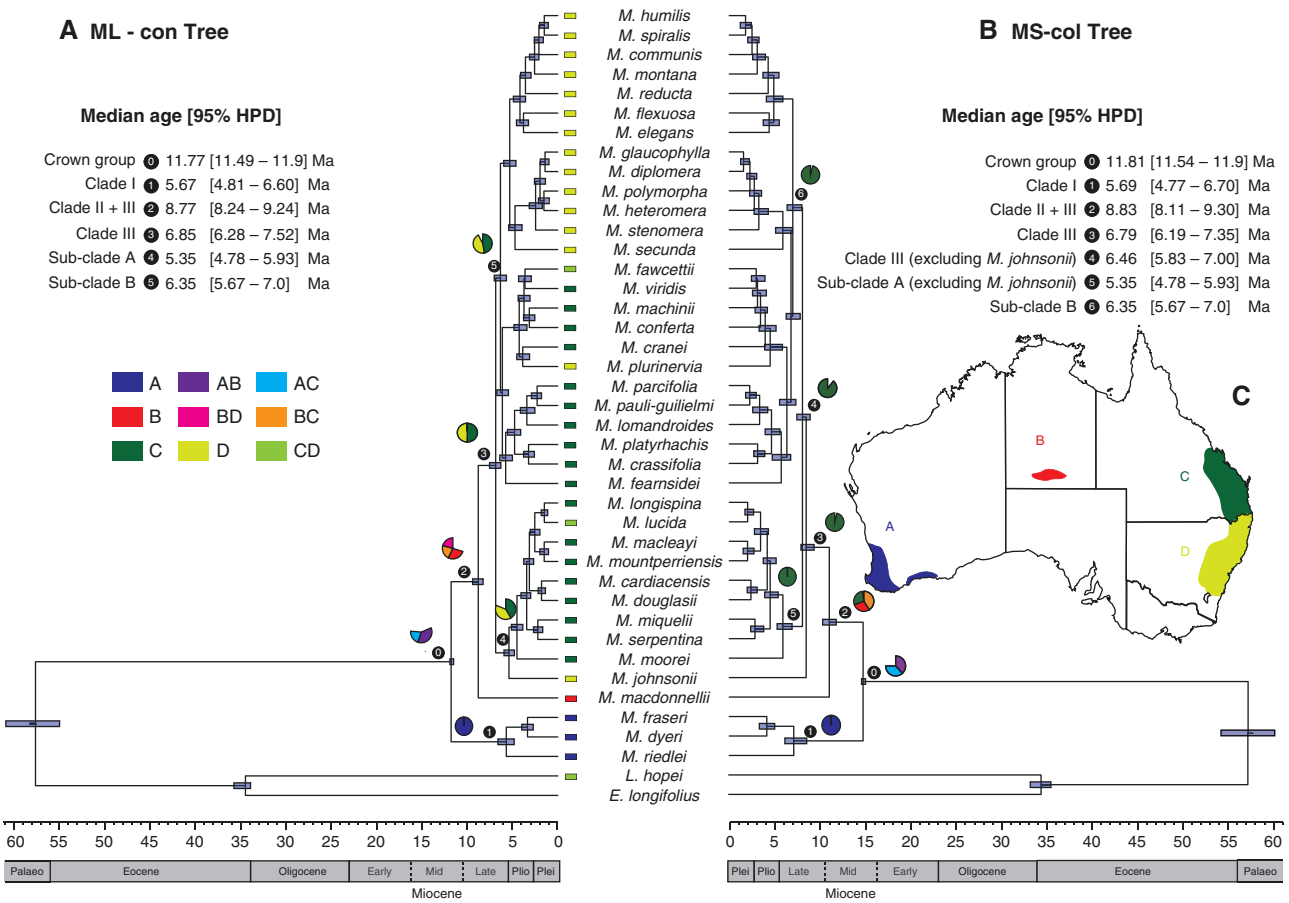

FIG. 3. Spatio-temporal diversification of the genus *Macrozamia* traced on ML-con (A) and MS-col (B) trees. Median ages of nodes of interest, with 95 % highest posterior density intervals (HPD), are given at the upper corner beside each tree. (C) Distribution map of *Macrozamia* in Australia based on four-area splits. Grey bars on the tree indicate 95 % HPD and pie charts indicate ancestral area of nodes of interest (>20 % only). Distribution information of each species is given with the taxon name.

node 4; Fig. 3B). In contrast, the ML-con time tree showed a relatively recent divergence of this species from the remaining taxa within sub-clade A of clade III around 4.5 Ma (95 % HPD: 3.85–5.11 Ma; Fig. 3A). Our results support the hypothesis that a mostly Miocene radiation occurred in the genus with an absolute rate of silent substitutions for *Macrozamia* at 2.0746 per site/billion years (Supplementary Data Fig. S4).

For ancestral area reconstruction, higher log-likelihood values were retrieved with three parameters in comparison to two parameters among the six models (Supplementary Data Table S1). This indicates a jump as an important pattern in the range variation of *Macrozamia*. BioGeoBEARS analyses showed DIVALIKE + j with the highest corrected AIC weight (AICc_wt) scores as the best-fit biogeographical model for ML-con and MS-col time trees (0.83 and 0.79, respectively). Thus, we only present the reconstruction of BioGeoBEARS under the DIVALIKE + j model (Fig. 3). The exact order of dispersal for the species of *Macrozamia* was unknown (node 0, Fig. 3). Based on the most likely ancestral range on each node, a total of seven (traced on the ML-con tree) or eight (traced on the MS-col tree) dispersal (speciation) events occurred across the four distinct areas of occurrence of the genus. The earliest dispersal event was estimated at the stem of clade II, followed by remaining events that occurred in eastern Australia (Areas C and D), within the last 7 Myr.

Ancestral state reconstruction

The likelihood inferences of six morphological characters based on the Mk1 model on the ML-con tree are shown in Figs 4 and 5. Among the three models implemented in ape, ER was the best fitting model for all the observed characters. Likelihood proportions for six key nodes of *Macrozamia* based on the Mk1 model and the ER models in R shown no well-supported (PP > 0.85) conflict, and congruent results were retrieved for most of the nodes (Supplementary Data Table S2).

Character state evolution revealed some homoplasy in each of the six morphological characters examined (Figs 4 and 5) with stem arborescence showing particularly high homoplasy (Fig. 4A). The ancestral state of stem arborescence for *Macrozamia* was uncertain due to the diversity of stem appearance among the major early-diverging clades, but was probably 'subterranean'. It was also the ancestral state for most of the other major nodes, with four and six independent shifts occurring from subterranean to an 'arborescent' or

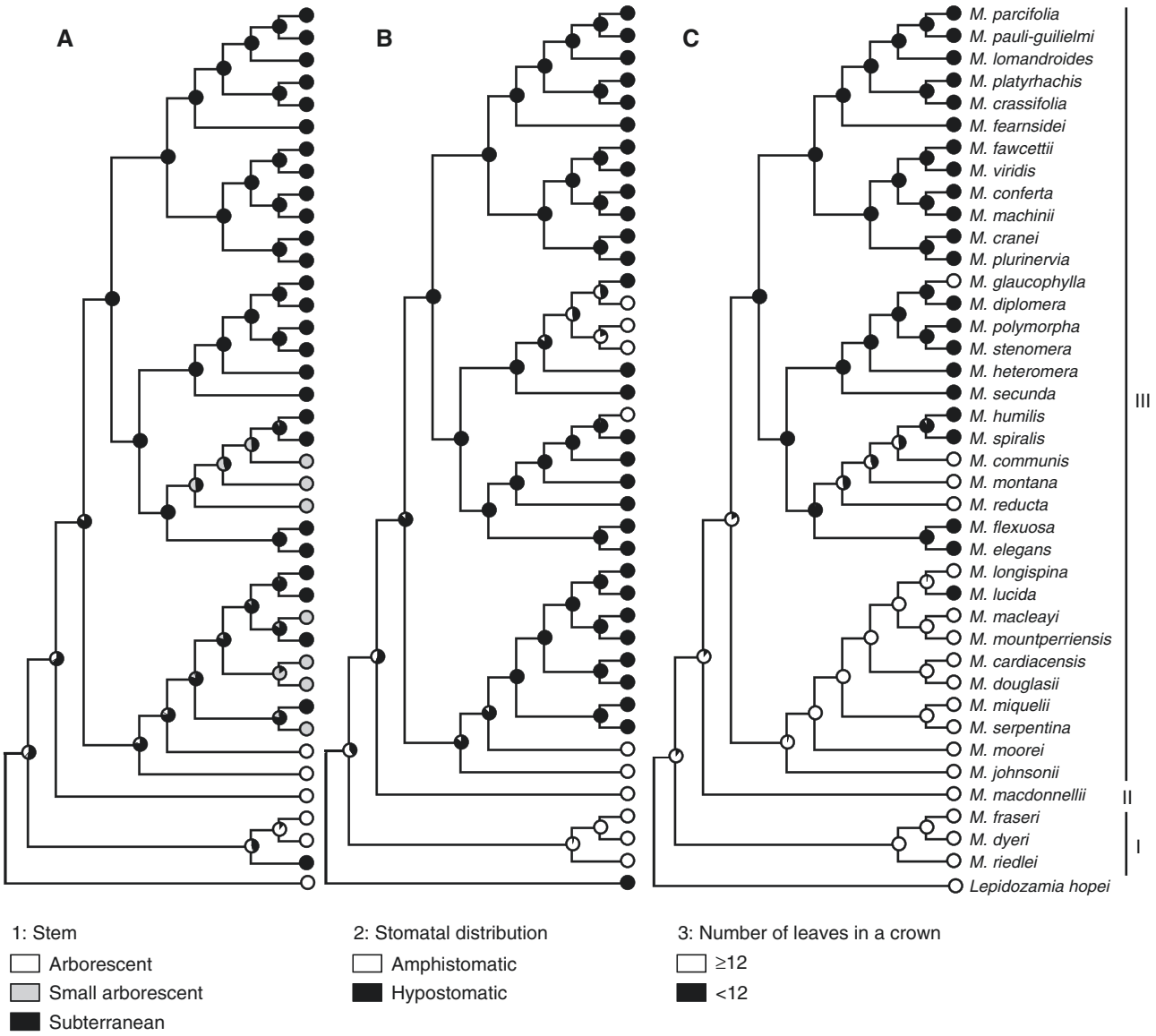

FIG. 4. Optimization of morphological characters: (A) stem, (B) stomatal distribution and (C) number of leaves in a crown, on ML trees of the concatenated dataset of SCGs. The pie chart at each node represents the probability of each character state for that morphological character.

'small arborescent' stem, respectively (Fig. 4A). Stomata distribution exhibited little homoplasy with an inferred shift from 'amphistomatic' ancestrally to 'hypostomatic' in clade III species (Fig. 4B). Moreover, '≥12' leaves arranged in the crown was the ancestral state in *Macrozamia* but shifted to '<12' leaves in species of sub-clade B of clade III. This character state also arose once in sub-clade A of clade III (Fig. 4C). Pinnacanth evolution was similarly complex, with pinnacanth present as the ancestral state in *Macrozamia* and with a shift to absence of pinnacanths in sub-clade B of clade III. Also, within sub-clade A, the absence of pinnacanths was inferred to have originated twice (Fig. 5A). 'Keeled' leaf rachis was the ancestral state is *Macrozamia*, and all other major nodes. Independent origins of 'flat' leaf rachis was also inferred once in clade I and three times in clade III (Fig. 5B). For seed colour, 'red' was the ancestral character state for *Macrozamia*, with independent shifts to orange-red seeds in sub-clade A of clade III, and orange-brown seeds in clade II (Fig. 5C).

DISCUSSION

Transcriptome-based phylogeny of Macrozamia

The present study showed that *Macrozamia* species, having plastid coding sequences and nuclear SCGs with few significant variable (<6 %) and parsimony-informative sites (<2 %), have highly conserved organellar and nuclear genomes. Mitochondrial and plastid genome assemblies of cycads revealed that cycad organellar genomes shared highly similar genomic profiles, accompanied by extremely slow evolution and mutation rates (Rai *et al.*, 2003; Chang *et al.*,

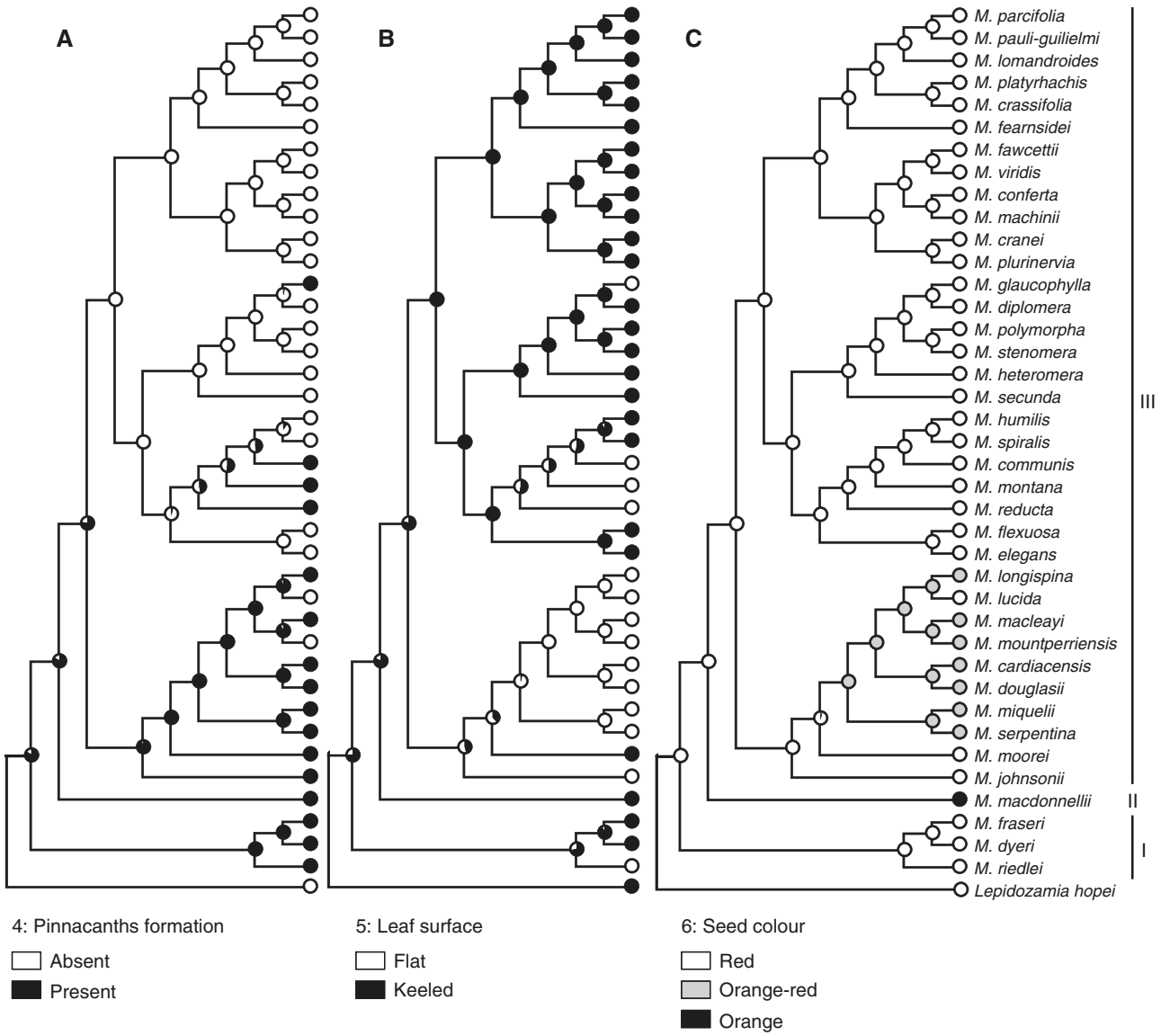

FIG. 5. Optimization of morphological characters: (A) pinnacanth formation, (B) leaf surface and (C) seed colour, on ML trees of the concatenated dataset of SCGs. The pie chart at each node represents the probability of each character state for that morphological character.

2020; Habib *et al.*, 2021). However, fairly well to highly supported topologies within the genus *Macrozamia* retrieved from SCGs for most branches indicated promising prospects for SCGs towards resolving phylogenetic relationships within cycads, in which organellar genomes were found to be relatively static. However, the phylogenetic relationships among some of the closely related species were not fully resolved, such as within sub-clade B of clade III. This is the first study to provide detailed insights into the evolutionary history of the genus. Noisy sequences, insufficient data, rapid diversification, hybridization and reticulate evolution have been considered to explain low resolution and incongruence in phylogenetic analyses (Sochor *et al.*, 2015; Spalink *et al.*, 2016; Y. Wang *et al.*, 2016). The SplitsTree network indicated that *M. johnsonii* shared edges with sub-clade A at a deep level near to the base (Supplementary Data Fig. S3). A network of shared edges occurred at both shallow and deep nodes within sub-clade B. This pattern indicated that ancient (in *M. johnsonii*), or both ancient to recent (in sub-clade B species) hybridization/introgression events occurred within *Macrozamia*. Furthermore, very short branches for conflicting topologies in ML-con and MS-col analyses (Fig. 2; Fig. S3) showed the possibility of incomplete lineage sorting (ILS) shaped the current phylogenetic pattern of the genus *Macrozamia*.

Spatio-temporal diversification of Macrozamia

The fossil calibrations of the current study followed the cycad phylogenomic and diversification analyses conducted by Condamine *et al.* (2015). The split between *Macrozamia* and its closest relatives *Lepidozamia* + *Encephalartos* occurred at around 57.62 Ma (95 % HPD: 46.2–69.1 Ma) during the late Palaeocene to early Eocene (Fig. 3). However, extant

Macrozamia species did not diversify until the late Miocene at about 11.77–11.8 Ma. Previous studies estimated the crown age of *Macrozamia* around 6 Ma (Crisp and Cook, 2011). The difference in node ages among the two studies occurred due differences in fossil calibrations and the low resolution of the markers used. However, both studies supported the hypothesis of mostly Miocene radiations in *Macrozamia*.

Long branches in phylogeny are usually hypothesized to be the consequence of extinction driven by climatic factors such as cooling/warming, and aridification (Crisp and Cook, 2011). This phenomenon is common in several gymnosperm lineages studied to date (Crisp and Cook, 2011; Stull *et al.*, 2021). The stem of the genus *Macrozamia* is also found to have a long branch, before the genus started its diversification around 11 Ma. The absolute rate of silent substitutions for *Macrozamia* was found to be significantly slower than that of angiosperms (Richardson *et al.*, 2013). The high level of sequence conservation within *Macrozamia* might imply either slow substitution rates in the genus, a short divergence time for the accumulation of molecular mutations or both. Australia was once dominated by mesic habitats, with much of its area covered by rainforests (Byrne *et al.*, 2011). The period of global cooling and drying started with the opening of a deep sea between Antarctica, Australia and South America at around 32 Ma (Hill and Brodribb, 1999; Zachos *et al.*, 2001; R. S. Hill, 2004). This led to the expansion of eremaean biomes (semi-arid and arid zones) in Australia, especially over the past 15–14 Myr. The expansion of the arid zone intensified during the Pliocene about 2–4 Ma (Kershaw *et al.*, 1994, 2005; Hill and Brodribb, 1999; Gallagher *et al.*, 2010; Byrne *et al.*, 2011). As a result, mesic-adapted taxa either became extinct, became restricted to less arid regions or adapted to the drier environments (R. S. Hill, 2004; Donoghue, 2008; Gallagher *et al.*, 2010). Significant extinctions have also been reported in other gymnosperms during the Cenozoic, especially around 29 and 16 Ma (Niklas, 1997; Crepet and Niklas, 2009).

The exact order of the diversification of *Macrozamia* is not resolved in the current study. *Macrozamia* species of eastern and western Australia underwent expansion and speciation at the same time at around 5–6 Ma, which was the time of increased aridification and expansion of eremaean biomes in Australia. Today, most of the mesic biomes are confined to the south-west western and eastern coasts of Australia (Byrne *et al.*, 2011). Species of *Macrozamia* occur in sclerophyll communities of these distantly located mesic biomes of Australia, except for *M. macdonnellii*, which is the only species distributed in MacDonnell Ranges and Mount Hay of central Australia, ~1300 km from its closest relatives in eastern Australia. This region is included in the eremaean biomes of Australia, but *M. macdonnellii* generally occurs in shaded areas on river banks, rocky steep slopes facing south, protected gulches and ravines (Ingham *et al.*, 2013). These provide the somewhat mesic micro-habitats required for successful survival of the species in this zone. Based on the current distribution pattern of the genus in three distinct areas, we suggest that *Macrozamia* was once widely distributed in Australia and underwent major extinction due to fluctuating climatic conditions such as cooling and mesic biomes undergoing contraction. Thus, extant *Macrozamia* species are persistent survivors of remnants of once widely distributed populations.

Today, the extant populations of *Macrozamia* species are largely restricted to refugia and are predicted to become increasingly isolated (Laidlaw and Forster, 2012). The dispersal-limited distributions of extant *Macrozamia* species probably occurred due to adult plant dependence on their obligate insect pollinators, lack of seed dispersal ability, exceptionally low seedling survival and shrinking habitats that were caused by past climatic perturbations and currently increasing ambient temperature (Laidlaw and Forster, 2012). Our findings further validated the concept that extant cycads clearly hold a complex history of ancient radiations, extraordinary stasis, major extinctions and recent species diversification.

Our results are consistent with several recent studies reporting recent divergence time estimates for the genera *Macrozamia*, *Lepidozamia* and *Encephalartos* (Ingham *et al.*, 2013; Condamine *et al.*, 2015; Mankga *et al.*, 2020; Y. Y.Liu *et al.*, 2022). However, some pollination biology data indicate these diverse extant cycads might be relicts dating back to the Late Cretaceous, i.e. before the separation of Australia and Africa as part of the Gondwanan landmass (see Mound and Terry, 2001; Labandeira *et al.*, 2007; Cai *et al.*, 2018). These contrasting hypotheses need to be addressed, perhaps with more newly discovered cycad fossils as well as incorporating geographical calibration points from tectonic evidence (J. Liu *et al.*, 2022).

Phylogeny in the context of traditional phenetic classification

Based on highly similar morphological affinities, species of *M.* sect. *Macrozamia* and *M.* sect. *Parazamia*t were further grouped into species complexes (Jones and Forster, 1994; K. D. Hill and Osborne, 2001; Jones *et al.*, 2001; Forster, 2004). Stem arborescence, stomatal distribution, number of leaves in a crown, pinnacanth formation, leaf surface appearance and seed colour have been traditionally used for these phenetic sectional classifications as well as the recognition of species complexes. The ancestral state reconstruction revealed the divergent evolution and homoplasy among the key morphological traits, because the traits examined herein were distributed across the phylogeny, and were not diagnostic for any clade (Figs 4 and 5). Nevertheless, the taxonomic classifications were partially congruent within our transcriptome-based phylogeny (Fig. 2).

Clade I. Species of clade I belong to the *M. riedlei* complex of *M.* sect. *Macrozamia*. These closely related species were characterized by rounded-slightly flattened petioles, amphistomatic leaflets and a distinct clear base to the petiole (Forster, 2004). Thus, *M.* sect. *Macrozamia* is now restricted to just three species, *M. riedlei*, *M. fraseri* and *M. dyeri*, and is sister to clades II and III.

Clade II. This clade includes only one species, *M. macdonnellii*, found disjunct in central Australia, and clade II is sister to clade III. According to traditional phenetic classification, *M. macdonnellii* shows close morphological affinities with *M. johnsonii* and *M. moorei* with all forming a species complex within *M.* sect. *Macrozamia* (Hill and Osborne, 2001; Forster, 2004). On the other hand, this species has also been considered to be related to clade I species because of its somewhat arid habitat, glaucous foliage and large seeds. The species is clearly distinct based on its semi-mesic habitat, distinct geographical

distribution, bluish green leaves, and largest seeds and ovulate cones among all the *Macrozamia* species (Hill and Osborne, 2001; Whitelock, 2002).

Clade III (sub-clade A). This clade included all species belonging to the *Macrozamia douglasii* complex along with two species of the *M. johnsonii* complex of *M.* sect. *Macrozamia sensu* Hill and Osborne (2001) (Fig. 2). *Macrozamia lucida* of *M.* sect. *Parazamia* is also in this clade. This species was proposed to be a taxonomically isolated species within *M.* sect. *Parazamia* (Hill and Osborne, 2001) and was only included in *M.* sect. *Parazamia* based on its small size. However, the number of leaves and the distinctive shape of the seed sclerotesta show its close affinity with the *M. douglasii* complex (Whitelock, 2002). All these species were closely placed in our phylogenetic reconstruction in clade III (sub-clade B); thus, those from *M.* sect. *Macrozamia* as circumscribed in Hill and Osborne (2001) are in an expanded monophyly concept of *M.* sect. *Parazamia* based on our results. All the species of *M.* sect. *Parazamia sensu* Hill and Osborne (2001) (except *M. lucida*) are in fact within sub-clade B of clade III. The phylogenetic positions of species complexes within *M.* sect. *Parazamia sensu* Hill and Osborne (2001) appear to be non-monophyletic in our analyses. Moreover, four species of the *Macrozamia reducta* complex of *M.* sect. *Macrozamia* (Hill and Osborne, 2001) are also within sub-clade B. However, the species of this complex are highly similar to other *M.* sect. *Macrozamia* species, especially the *M. douglasii* complex. However, these medium-sized cycads differed from all other species based on their distribution being restricted to New South Wales, and having broad based spines (5–12 mm) on the ovulate sporophylls (Hill and Osborne, 2001; Forster, 2004). Overall, the validity of sectional divisions of the genus *Macrozamia* is inconsistent with the current phylogenetic framework. Importantly, it is the poorly supported relationship among species complexes of *M.* sect. *Parazamia* that has highlighted the potential problems regarding the infraspecific taxa. For example, how many species are to be recognized and what is a supported infrageneric classification? What is clear is that *M.* sect. *Macrozamia*, as represented by clade I, is reduced from 16 species (Hill and Osborne, 2001) to three species. The 13 excluded species are found as one comprising clade II (*M. macdonnellii*) and 12 as part of clade III. Of the latter, nine species are placed in sub-clade A. Note that of these nine, *M. serpentina* was described after K. D. Hill (1998) and Hill and Osborne (2001) but placed in *M.* sect. *Macrozamia* by Jones *et al.* (2001) when they published the species description. Similarly, although *M. macleayi* is considered a synonym of *M. miquelii* by K. D. Hill (1998) and not included in Hill and Osborne (2001), it is recognized as a species in *M.* sect. *Macrozamia* by Jones *et al.* (2001). Thus, sub-clade A, with the exception of *M. lucida*, consists of species from *M.* sect. *Macrozamia.* Interestingly, the other three species, *M. reducta, M. montana* and *M. communis*, form a grade within sub-clade B in the *M. reducta* complex. Therefore, it appears that the species formerly placed in *M.* sect. *Macrozamia* do form a monophyletic group sub-clade A and a grade within sub-clade B. Thus, those species formerly placed in *M.* sect. *Macrozamia* are not widely dispersed within the phylogeny but rather just show new placements as related units within *M.* sect. *Parazamia.*

The three major clades of *Macrozamia* recognized in our study could not be explained based solely on morphological characters or by biogeographical evidence, but rather a combination of the two. East Australian species of *Macrozamia* that have been considered to have morphological affinities with *M.* sect. *Macrozamia sensu* Hill and Osborne (2001) (here sub-clade A) and *M.* sect. *Parazamia sensu* Hill and Osborne (2001) (here sub-clade B) are found, in our analyses, to be part of sub-clade A and sub-clade B in a broader concept of the section represented by clade III. We consider limited dispersal events have occurred within this area. Johnson (1959) proposed that species of *M.* sect. *Parazamia* are actually the descendants of *M.* sect. *Macrozamia* through evolutionary transitions in the rate or timing of a developmental pathway (i.e. neoteny, a type of pedomorphosis). Pedomorphosis or neotenous reduction of plant body architecture as a persistent juvenile stage has also been reported in other vascular plant groups (Bogner, 2009; Geuten and Coenen, 2013; F-G. Wang *et al.*, 2014; W. Wang *et al.*, 2014; Bruy, 2018). Within cycads, Chrysler (1937) indicated that tuberous species of *Zamia* and *Stangeria* are persistent juveniles in some of their vascular tissues and habit that occurred in times and regions of climatic stress. Other genera of cycads such as *Ceratozamia* and *Encephalartos* could also have undergone similar developments because they have both arborescent and subterranean species. Brough and Taylor (1940) reported that leaves in *Macrozamia communis* showed extremely slow production and they might take around 10–12 years to shed the juvenile foliage. In that case, young populations would be at risk from repeated fires. Hence, neotenic events could provide early reproductive maturity with the vegetative shoot remaining subterranean and prevent repeated geographical disturbances. Close placement of *M. communis*, *M. montana* and *M. reducta* of *M.* sect. *Macrozamia sensu* Hill and Osborne (2001) with *M.* sect. *Parazamia* species (sub-clade B of clade III) might be the result of neotenic events that occurred in their immediate ancestors. Carpenter (1991) mentioned the possibility of neotenic events in *Macrozamia* based on shared cuticular characters among *Macrozamia diplomera* (*M.* sect. *Macrozamia*), *M. heteromera* and *M. stenomera* (*M.* sect. *Parazamia*). These are geographically proximal species and are closely placed in our phylogenetic tree (Figs 2 and 3 and Supplementary Data Fig. S3). This evidence along with the close phylogenetic placement of morphologically distinct species of *Macrozamia* in this study supports the hypothesis of possible neotenic events as resulting in the evolutionary relationships within the genus.

CONCLUSION

Based on extensive taxon sampling (39/41 taxa) and a transcriptome dataset of 4740 single-copy nuclear genes, we reconstructed a well-resolved phylogeny for *Macrozamia*. The genus contains three major clades corresponding to their distribution in three areas of endemism. Extant species of *Macrozamia* have been the result mostly of Miocene radiations. Based on the phylogenetic and biogeographical pattern of *Macrozamia*, we predicted that the genus experienced extinctions due to historical climatic factors such as aridification, mesic biome decline and lack of long-distance dispersal

ability. The spatio-temporal diversification pattern of the genus *Macrozamia* revealed in this study will provide a gateway to study the processes responsible for pollination mutualism and co-diversification of *Macrozamia* species, and their obligate insect pollinators.

SUPPLEMENTARY DATA

Supplementary data are available online at https://academic.oup.com/aob and consist of the following. Figure S1: Phylogenetic reconstruction of 39 *Macrozamia* and two outgroup taxa with a concatenated dataset of 40 plastid protein coding genes from the nucleotide dataset. Figure S2: Species trees of the genus *Macrozamia* generated with ASTRAL-III analyses of the nucleotide dataset. Figure S3: A phylogenetic network of the concatenated dataset of 39 *Macrozamia* species generated using SplitsTree5. Figure S4: Synonymous and non-synonymous trees for *Macrozamia*. Table S1: Best fitting model estimation in BioGeoBEARS. Table S2: Comparison of ancestral state probability with the mk1 model in Mesquite and best fitting model in APE.

ACKNOWLEDGEMENTS

S.H. and S.Z. conceived the experimenst; A.L. and Y.G. performed the experiments and collected the data; S.H., S.D., D.W.S., Y.L. and Y.G. performed data analyses; S.H. drafted the manuscript and revised it with input from all the authors. We acknowledge Nong Nooch Tropical Botanical Garden, Thailand, especially the President Kampon Tansacha for providing fully documented material for this study. Wang Wei, Chenyang Cai and José Said Gutiérrez-Ortega are thanked for insightful discussions and valuable comments that greatly improved the manuscript.

FUNDING

This study was supported by the Scientific Foundation of Urban Management Bureau of Shenzhen (Nos. 202019 and 202208 to S.Z., No. 202105 to Y.Q., No. 202106 to S.D.), and the Biodiversity Survey and Assessment Project of the Ministry of Ecology and Environment, China (No. 2019HJ2096001006 to S.Z. and Y.L.).

LITERATURE CITED

Abascal F, **Zardoya R**, **Telford MJ. 2010**. TranslatorX: multiple alignment of nucleotide sequences guided by amino acid translations. *Nucleic Acids Research* **38**: W7–13.

Ali MA, **Rahman MO**, **Lee J**, ***et al***. **2020**. Dissecting molecular evolutionary relationship of Krameriaceae inferred from phylotranscriptomic analysis. *Bangladesh Journal of Plant Taxonomy* **27**: 427–433.

Bogner J. 2009. The free-floating Aroids (Araceae)–living and fossil. *Zitteliana* **48**: 113–128.

Brenner ED, **Stevenson DW**, **Twigg RW. 2003a**. Cycads: evolutionary innovations and the role of plant-derived neurotoxins. *Trends in Plant Science* **8**: 446–452.

Brenner ED, **Stevenson DW**, **McCombie RW**, ***et al***. **2003b**. Expressed sequence tag analysis in *Cycas*, the most primitive living seed plant. *Genome Biology* **4**: 1–11.

Brookes D, **Hereward J**, **Terry L**, **Walter G. 2015**. Evolutionary dynamics of a cycad obligate pollination mutualism–Pattern and process in extant *Macrozamia* cycads and their specialist thrips pollinators. *Molecular Phylogenetics and Evolution* **93**: 83–93.

Brough P, **Taylor M. 1940**. An investigation of the life cycle of *Macrozamia spiralis* Miq. *Proceedings of the Linnean Society of New South Wales* **65**:494–524.

Bruy D. 2018. *Diversity, ecology and evolution of monocaulous plants in New Caledonia*. Université Montpellier.

Byrne M, **Steane DA**, **Joseph L**, ***et al***. **2011**. Decline of a biome: evolution, contraction, fragmentation, extinction and invasion of the Australian mesic zone biota. *Journal of Biogeography* **38**: 1635–1656.

Cai C, **Escalona HE**, **Li L**, **Yin Z**, **Huang D**, **Engel MS. 2018**. Beetle pollination of cycads in the Mesozoic. *Current Biology* **28**: 2806–2812.e1.

Calonje M, **Meerow AW**, **Griffith MP**, ***et al***. **2019**. A time-calibrated species tree phylogeny of the New World cycad genus *Zamia* L. (Zamiaceae, Cycadales). *International Journal of Plant Sciences* **180**: 286–314.

Caputo P, **Cozzolino S**, **Luca Pd**, **Moretti A**, **Stevenson D. 2004**. Molecular phylogeny of Zamia (Zamiaceae). In: **Walters T**, **Osborne R**, eds. *Cycad classification: Concepts and recommendations*. Wallingford: CABI Publishing, 149–157.

Carpenter RJ. 1991. *Macrozamia* from the early Tertiary of Tasmania and a study of the cuticles of extant species. *Australian Systematic Botany* **4**: 433–444.

Chang ACG, **Lai Q**, **Chen T**, ***et al***. **2020**. The complete chloroplast genome of *Microcycas calocoma* (Miq.) A. DC.(Zamiaceae, Cycadales) and evolution in Cycadales. *PeerJ* **8**: e8305.

Chrysler M. 1937. Persistent juveniles among the cycads. *Botanical Gazette* **98**: 696–710.

Clugston JAR, **Griffith MP**, **Kenicer GJ**, ***et al***. **2016**. *Zamia* (Zamiaceae) phenology in a phylogenetic context: does in situ reproductive timing correlate with ancestry? *Edinburgh Journal of Botany* **73**: 345–370.

Condamine FL, **Nagalingum NS**, **Marshall CR**, **Morlon H. 2015**. Origin and diversification of living cycads: a cautionary tale on the impact of the branching process prior in Bayesian molecular dating. *BMC Evolutionary Biology* **15**: 1–18.

Crepet WL, **Niklas KJ. 2009**. Darwin's second 'abominable mystery': why are there so many angiosperm species? *American Journal of Botany* **96**: 366–381.

Crisp MD, **Cook LG. 2011**. Cenozoic extinctions account for the low diversity of extant gymnosperms compared with angiosperms. *New Phytologist* **192**: 997–1009.

Daly D, **Cameron K**, **Stevenson D. 2001**. Plant systematics in the age of genomics. *Plant Physiology* **127**: 1328–1333.

De Castro O, **Vázquez-Torres M**, **De Luca P. 2006**. Utility of AFLP markers for the assessment of molecular relationships in *Ceratozamia* Brongn. (Zamiaceae). *Plant Biosystems* **140**: 221–228.

Donoghue MJ. 2008. A phylogenetic perspective on the distribution of plant diversity. *Proceedings of the National Academy of Sciences* **105**: 11549–11555.

Dorsey BL, **Gregory TJ**, **Sass C**, **Specht CD. 2018**. Pleistocene diversification in an ancient lineage: a role for glacial cycles in the evolutionary history of *Dioon* Lindl. (Zamiaceae). *American Journal of Botany* **105**: 1512–1530.

Emms DM, **Kelly S. 2019**. OrthoFinder: phylogenetic orthology inference for comparative genomics. *Genome Biology* **20**: 1–14.

Forster P. 2004. Classification concepts in *Macrozamia* (Zamiaceae) from eastern Australia. In: **Walters T**, **Osborne R**, eds. *Cycad classification: concepts and recommendations*. Wallingford: CABI Publishing, 85–94.

Gallagher RV, **Beaumont LJ**, **Hughes L**, **Leishman MR. 2010**. Evidence for climatic niche and biome shifts between native and novel ranges in plant species introduced to Australia. *Journal of Ecology* **98**: 790–799.

Geuten K, **Coenen H. 2013**. Heterochronic genes in plant evolution and development. *Frontiers in Plant Science* **4**: 381–381.

González D, **Vovides AP**, **Bárcenas C. 2008**. Phylogenetic relationships of the Neotropical genus Dioon (Cycadales, Zamiaceae) based on nuclear and chloroplast DNA sequence data. *Systematic Botany* **33**: 229–236.

Grabherr MG, **Haas BJ**, **Yassour M**, ***et al***. **2011**. Full-length transcriptome assembly from RNA-Seq data without a reference genome. *Nature Biotechnology* **29**: 644–652.

Gutiérrez-Ortega JS, **Salinas-Rodríguez MM**, **Martínez JF**, ***et al***. **2018**. The phylogeography of the cycad genus *Dioon* (Zamiaceae) clarifies its

Cenozoic expansion and diversification in the Mexican transition zone. *Annals of Botany* **121**: 535–548.
Habib S, **Dong S**, **Liu Y**, **Liao W**, **Zhang S. 2021**. The complete mitochondrial genome of *Cycas debaoensis* revealed unexpected static evolution in gymnosperm species. *PLoS One* **16**: e0255091.
Helfrich P, **Rieb E**, **Abrami G**, **Lücking A**, **Mehler A. 2018**. TreeAnnotator: versatile visual annotation of hierarchical text relations. Proceeding of the Eleventh International Conference. Language Resources and Evaluation (LREC). European Language Resources Associatioon (ELRA).
Hill KD. 1998. Cycadophyta. *Flora of Australia* **48**: 597–661.
Hill RS. 2004. Origins of the southeastern Australian vegetation. *Philosophical Transactions of the Royal Society B: Biological Sciences* **359**: 1537–1549.
Hill RS, **Brodribb TJ. 1999**. Southern conifers in time and space. *Australian Journal of Botany* **47**: 639–696.
Hill KD, **Osborne R. 2001**. *Cycads of Australia*. Nashville, TN: Kangaroo Press.
Huson DH. 1998. SplitsTree: analyzing and visualizing evolutionary data. *Bioinformatics* **14**: 68–73.
Huson DH, **Bryant D. 2006**. Application of phylogenetic networks in evolutionary studies. *Molecular Biology and Evolution* **23**: 254–267.
Ingham JA, **Forster PI**, **Crisp MD**, **Cook LG. 2013**. Ancient relicts or recent dispersal: how long have cycads been in central Australia? *Diversity and Distributions* **19**: 307–316.
IUCN. **2022**. *The IUCN Red List of Threatened Species. Version 2022-1*. https://www.iucnredlist.org (29 July 2022, date last accessed).
Johnson LA. 1959. *The families of cycads and the Zamiaceae of Australia*. Sydney: Linnean Society.
Johnson MG, **Gardner EM**, **Liu Y**, ***et al***. **2016**. HybPiper: extracting coding sequence and introns for phylogenetics from high-throughput sequencing reads using target enrichment. *Applications in Plant Sciences* **4**: 1600016.
Jones DL, **Forster PI. 1994**. Seven new species of *Macrozamia* section *Parazamia* (Miq.) Miq. (*Zamiaceae* section *Parazamia*) from Queensland. *Austrobaileya* **4**: 269–288.
Jones DL, **Forster PI**, **Sharma IK. 2001**. Revision of the *Macrozamia miquelii* (F.Muell.) A.DC. (Zamiaceae section *Macrozamia*) group. *Austrobaileya* **6**: 67–94.
Kalyaanamoorthy S, **Minh BQ**, **Wong TK**, **Von Haeseler A**, **Jermiin LS. 2017**. ModelFinder: fast model selection for accurate phylogenetic estimates. *Nature Methods* **14**: 587–589.
Katoh K, **Standley DM. 2013**. MAFFT multiple sequence alignment software version 7: improvements in performance and usability. *Molecular Biology and Evolution* **30**: 772–780.
Kershaw AP, **Martin H**, **Mason JM. 1994**. The Neogene: a period of transition. In: *History of the Australian vegetation: Cretaceous to Recent*, 299.
Kershaw AP, **Moss PT**, **Wild R. 2005**. Patterns and causes of vegetation change in the Australian Wet Tropics region over the last 10 million years. In: *Tropical rainforests: past, present and future*, 374–400.
Labandeira CC, **Kvaček J**, **Mostovski MB. 2007**. Pollination drops, pollen, and insect pollination of Mesozoic gymnosperms. *Taxon* **56**: 663–695.
Laetsch DR, **Blaxter ML. 2017**. KinFin: software for taxon-aware analysis of clustered protein sequences. *G3: Genes, Genomes, Genetics* **7**: 3349–3357.
Laidlaw MJ, **Forster PI. 2012**. Climate predictions accelerate decline for threatened *Macrozamia* cycads from Queensland, Australia. *Biology* **1**: 880–894.
Leebens-Mack JH, **Barker MS**, **Carpenter EJ**, ***et al***. **2019**. One thousand plant transcriptomes and the phylogenomics of green plants. *Nature* **574**: 679–685.
Lewis PO. 2001. A likelihood approach to estimating phylogeny from discrete morphological character data. *Systematic Biology* **50**: 913–925.
Liu J, **Zhang S**, **Nagalingum N**, **Chiang Y-C**, **Lindstrom A**, **Xun G. 2018**. Phylogeny of the gymnosperm genus *Cycas* L. (Cycadaceae) as inferred from plastid and nuclear loci based on a large-scale sampling: evolutionary relationships and taxonomical implications. *Molecular Phylogenetics and Evolution* **127**:87–97.
Liu YY, **Jin WT**, **Wei XX**, **Wang XQ. 2022**. Phylotranscriptomics reveals the evolutionary history of subtropical East Asian white pines: further insights into gymnosperm diversification. *Molecular Phylogenetics and Evolution* **168**: 107403.
Liu J, **Lindstrom AJ**, **Marler TE**, **Gong X. 2022**. Not that young: combining plastid phylogenomic, plate tectonic and fossil evidence indicates a Palaeogene diversification of Cycadaceae. *Annals of Botany* **129**: 217–230.
Liu Y, **Wang S**, **Li L**, ***et al***. **2022**. The *Cycas* genome and the early evolution of seed plants. *Nature Plants* **8**: 389–401.
Ladiges PY, **Kellermann J**, **Nelson G**, **Humphries CJ**, **Udovicic F. 2005**. Historical biogeography of Australian Rhamnaceae, tribe Pomaderreae. *Journal of Biogeography* **32**: 1909–1919.
Maddison WP, **Maddison DR. 2021**. *Mesquite: A Modular System for Evolutionary Analysis. Version 3.70*. http://www.mesquiteproject.org.
Mankga LT, **Yessoufou K**, **Chitakira M. 2020**. On the origin and diversification history of the African genus *Encephalartos*. *South African Journal of Botany* **130**: 231–239.
Matzke N. 2018. *BioGeoBEARS: BioGeography with Bayesian (and likelihood) evolutionary analysis with R scripts. version 1.1. 1*. San Francisco, CA: GitHub. https://github.com/nmatzke/BioGeoBEARS.
Medina-Villarreal A, **González-Astorga J**, **de Los Monteros AE. 2019**. Evolution of *Ceratozamia* cycads: a proximate-ultimate approach. *Molecular Phylogenetics and Evolution* **139**: 106530.
Minh BQ, **Schmidt HA**, **Chernomor O**, ***et al***. **2020**. IQ-TREE 2: new models and efficient methods for phylogenetic inference in the genomic era. *Molecular Biology and Evolution* **37**: 1530–1534.
Mound LA, **Terry I. 2001**. Thrips pollination of the central Australian cycad, *Macrozamia macdonnellii* (Cycadales). *International Journal of Plant Sciences* **162**: 147–154.
Moynihan J, **Stevenson D**, **Lewis CE**, **Vovides AP**, **Caputo P**, **Francisco-Ortega J. 2012**. A phylogenetic study of *Dioon* Lind.(Zamiaceae, Cycadales), based on morphology, nuclear ribosomal DNA, a low copy nuclear gene and plastid RFLPs. *Memoirs of the New York Botanical Garden* **106**: 448–479.
Muse SV, **Gaut BS. 1994**. A likelihood approach for comparing synonymous and nonsynonymous nucleotide substitution rates, with application to the chloroplast genome. *Molecular Biology and Evolution* **11**: 715–724.
Niklas KJ. 1997. *The evolutionary biology of plants*. Chicago: University of Chicago Press.
Osborne R, **Calonje M**, **Hill KD**, **Stanberg L**, **Stevenson D. 2012**. The world list of cycads. *Memoirs of the New York Botanical Garden* **106**: 480–510.
Paradis E, **Claude J**, **Strimmer K. 2004**. APE: analyses of Phylogenetics and Evolution in R language. *Bioinformatics* **20**: 289–290.
Pond SL, **Kosakovsky F**, **Simon DW**, **Muse SV. 2005**. Hyphy: hypothesis testing using phylogenies. *Bioinformatics Biological Insights* **21**: 676–679.
Rai HS, **O'Brien HE**, **Reeves PA**, **Olmstead RG**, **Graham SW. 2003**. Inference of higher-order relationships in the cycads from a large chloroplast data set. *Molecular Phylogenetics and Evolution* **29**: 350–359.
Richardson AO, **Rice DW**, **Young GJ**, **Alverson AJ**, **Palmer JD. 2013**. The 'fossilized' mitochondrial genome of *Liriodendron tulipifera*: ancestral gene content and order, ancestral editing sites, and extraordinarily low mutation rate. *BMC Biology* **11**: 1–17.
Salas-Leiva DE, **Meerow AW**, **Calonje M**, ***et al***. **2013**. Phylogeny of the cycads based on multiple single-copy nuclear genes: congruence of concatenated parsimony, likelihood and species tree inference methods. *Annals of Botany* **112**: 1263–1278.
Sanderson MJ. 2002. Estimating absolute rates of molecular evolution and divergence times: a penalized likelihood approach. *Molecular Biology and Evolution* **19**: 101–109.
Sangin P, **Forster PI**, **Mingmuang M**, **Kokubugata G. 2008**. A phylogeny for two cycad families (Stangeriaceae and Zamiaceae) based on chloroplast DNA sequences. *Bulletin of the National Museum of Nature and Science. Series B. Botany* **34**: 75–82.
Sharma I, **Jones D**, **Forster P**, **Young A. 1998**. The extent and structure of genetic variation in the *Macrozamia pauli-guilielmi* complex (Zamiaceae). *Biochemical Systematics and Ecology* **26**: 45–54.
Sharma I, **Jones D**, **Forster P. 1999a**. Contribution of isozymic analysis in differentiating *Macrozamia moorei* DL Jones and KD Hill from *M. johnsonii* F. Muell (Zamiaceae). *Austrobaileya* **5**: 363–365.
Sharma I, **Jones D**, **Forster P**, **Young A. 1999b**. Low isozymic differentiation among five species of the *Macrozamia heteromera* group (Zamiaceae). *Biochemical Systematics and Ecology* **27**: 67–77.
Sharma I, **Jones D**, **Forster P. 2004**. Genetic differentiation and phenetic relatedness among seven species of the *Macrozamia plurinervia* complex (Zamiaceae). *Biochemical Systematics and Ecology* **32**: 313–327.
Shen W, **Le S**, **Li Y**, **Hu F. 2016**. SeqKit: a cross-platform and ultrafast toolkit for FASTA/Q file manipulation. *PLoS One* **11**: e0163962.
Smith SA, **O'Meara BC. 2012**. treePL: divergence time estimation using penalized likelihood for large phylogenies. *Bioinformatics* **28**: 2689–2690.

Sochor M, **Vašut RJ**, **Sharbel TF**, **Trávníček B. 2015**. How just a few makes a lot: speciation via reticulation and apomixis on example of European brambles (*Rubus* subgen. *Rubus*, Rosaceae). *Molecular Phylogenetics and Evolution* **89**: 13–27.

Spalink D, **Drew BT**, **Pace MC**, ***et al***. **2016**. Evolution of geographical place and niche space: patterns of diversification in the North American sedge (Cyperaceae) flora. *Molecular Phylogenetics and Evolution* **95**: 183–195.

Stamatakis A. 2014. RAxML version 8: a tool for phylogenetic analysis and post-analysis of large phylogenies. *Bioinformatics* **30**: 1312–1313.

Stull GW, **Qu XJ**, **Parins-Fukuchi C**, ***et al***. **2021**. Gene duplications and phylogenomic conflict underlie major pulses of phenotypic evolution in gymnosperms. *Nature Plants* **7**: 1015–1025.

Talavera G, **Castresana J. 2007**. Improvement of phylogenies after removing divergent and ambiguously aligned blocks from protein sequence alignments. *Systematic Biology* **56**: 564–577.

Terry I, **Walter GH**, **Moore C**, **Roemer R**, **Hull C. 2007**. Odor-mediated push-pull pollination in cycads. *Science* **318**: 70–70.

Terry I, **Roemer R**, **Walter GH**, **Booth D. 2014**. Thrips' responses to thermogenic associated signals in a cycad pollination system: the interplay of temperature, light, humidity and cone volatiles. *Functional Ecology* **28**: 857–867.

Treutlein J, **Vorster P**, **Wink M. 2005**. Molecular relationships in *Encephalartos* (Zamiaceae, Cycadales) based on nucleotide sequences of nuclear *ITS* 1&2, *rbcL*, and genomic ISSR fingerprinting. *Plant Biology* **7**: 79–90.

Wang F-G, **Barratt S**, **Falcon W**, ***et al***. **2014**. On the monophyly of subfamily Tectarioideae (Polypodiaceae) and the phylogenetic placement of some associated fern genera. *Phytotaxa* **164**: 1–16.

Wang W, **Haberer G**, **Gundlach H**, ***et al***. **2014**. The *Spirodela polyrhiza* genome reveals insights into its neotenous reduction fast growth and aquatic lifestyle. *Nature Communications* **5**: 3311.

Wang Y, **Chen Q**, **Chen T**, **Tang H**, **Liu L**, **Wang X. 2016**. Phylogenetic insights into Chinese *Rubus* (Rosaceae) from multiple chloroplast and nuclear DNAs. *Frontiers in Plant Science* **7**: 968–968.

Wen J, **Xiong Z**, **Nie Z-L**, ***et al***. **2013**. Transcriptome sequences resolve deep relationships of the grape family. *PLoS One* **8**: e74394.

Wen J, **Yu Y**, **Xie D-F**, ***et al***. **2020**. A transcriptome-based study on the phylogeny and evolution of the taxonomically controversial subfamily Apioideae (Apiaceae). *Annals of Botany* **125**: 937–953.

Whitelock LM. 2002. *The cycads.* Portland, OR: Timber Press.

Xiao L-Q, **Möller M**, **Zhu H. 2010**. High nrDNA ITS polymorphism in the ancient extant seed plant *Cycas*: incomplete concerted evolution and the origin of pseudogenes. *Molecular Phylogenetics and Evolution* **55**: 168–177.

Yang X, **Cheng Y-F**, **Deng C**, ***et al***. **2014**. Comparative transcriptome analysis of eggplant (*Solanum melongena* L.) and turkey berry (*Solanum torvum* Sw.): phylogenomics and disease resistance analysis. *BMC Genomics* **15**: 1–13.

Zachos JC, **Mo P**, **Sloan LC**, **Thomas E**, **Billups K. 2001**. Trends, rhythms, and aberrations in global climate 65 Ma to present. *Science* **292**: 686–693.

Zhang C, **Rabiee M**, **Sayyari E**, ***et al***. **2018**. ASTRAL-III: polynomial time species tree reconstruction from partially resolved gene trees. *BMC Bioinformatics* **19**: 153.

Zhang C, **Huang CH**, **Liu M**, ***et al***. **2021**. Phylotranscriptomic insights into Asteraceae diversity, polyploidy, and morphological innovation. *Journal of Integrative Plant Biology* **63**: 1273–1293.

Zumajo-Cardona C, **Frangos S**, **Stevenson D. 2021a**. Seed anatomy and development in Cycads and *Ginkgo*, keys for understanding the evolution of seeds. *Flora* **285**: 151951.

Zumajo-Cardona C, **Little DP**, **Stevenson D**, **Ambrose BA. 2021b**. Expression analyses in *Ginkgo biloba* provide new insights into the evolution and development of the seed. *Scientific Reports* **11**: 21995.